RESEARCH ARTICLE

Open Access

Isolation, characterization, and transcriptome profiling of umbilical cord mesenchymal stem cells in pigs

2024 Volume 1, Article number: e008

https://doi.org/10.48130/animadv-0024-0008

Received: 27 August 2024

Revised: 2 November 2024

Accepted: 12 November 2024

Published online: 13 December 2024

Bienvenu Odjoubiré Mahougnon Koutonin[1], Fuyao Zhang[1], Yuan Jiang[1], Chao Jia[1], Hussain Ahmad Saeed[1], Yanfeng Fu[2], Honglin Liu[1], Camus Mahougnon Adoligbe[3] and Juan Li[1*]

[1] College of Animal Science and Technology, Nanjing Agricultural University, Nanjing 210095, China
[2] Institute of Animal Science, Jiangsu Academy of Agricultural Sciences, Nanjing 210095, China
[3] Research Unit on Communicable Diseases, Department of Animal Production and Health, Polytechnic School of Abomey-Calavi, University of Abomey-Calavi, 01bp 2009, Cotonou, Benin
* Corresponding author, E-mail: juanli@njau.edu.cn

Abstract

Given the high rate of proliferation and capacity for multipotent differentiation, mesenchymal stem cells (MSCs) are essential for the treatment of diseases and cell therapy. To understand the properties of porcine umbilical cord MSCs (pUC-MSCs) across time, this study assessed the cells at many stages (P4, P6, P9, and P11). The cells showed an 'S' shaped growth curve, a population doubling time of 23 h, and fibroblast-like morphology along with significant proliferative ability. P4 and P6 displayed more CD90-positive cells than P9 and P11, demonstrating that they retained the usual MSC surface markers. The study discovered 132 differentially expressed genes (DEGs) associated with cell differentiation and 127 associated with stemness by transcriptome analysis using RNA sequencing (RNA-seq). Important stemness genes such as *APC, KRAS*, and *SMAD5* were expressed more strongly in P6, however, stemness markers were reduced in P9 and P11, showing that as cells became older, they shifted towards differentiation which we also confirmed with differentiation markers such as *NOTCH3, MAPK8, OCT4, SOX2, and NANOG*. Considerable enrichment of biological processes and molecular functions was found in P6 compared to P4 by gene ontology (GO) and KEGG pathway analysis, with a noticeable reduction in later passages. Based on this study, pUC-MSCs retain greater stemness in the early passages (P4 and P6), but the later passages (P9 and P11) exhibit decreased regeneration capacity due to a loss of stemness and an increase in differentiation markers. This emphasizes how vital it is to choose the right cell passages for applications in regenerative medicine, where the ability to maintain stemness is essential for effective treatment.

Citation: Koutonin BOM, Zhang F, Jiang Y, Jia C, Saeed HA, et al. 2024. Isolation, characterization, and transcriptome profiling of umbilical cord mesenchymal stem cells in pigs. *Animal Advances* 1: e008 https://doi.org/10.48130/animadv-0024-0008

Introduction

MSCs represent a paradigm shift in regenerative medicine and offer enormous potential for tissue repair and therapeutic applications. These multipotent cells, characterized by their ability to self-renew and differentiate into various cell lineages, have attracted considerable attention due to their versatility. The evolution of MSC research spans multiple species, including humans, pigs, cattle, and rodents, highlighting the diverse types and sources of MSCs that make unique contributions to the field[1]. MSCs have been isolated and characterized from various tissue sources such as bone marrow, adipose tissue, and umbilical cords in multiple species. MSCs have shown promise in human regenerative medicine, particularly in tissue and organ repair therapies. For example, MSCs have shown potential in periodontal regeneration, with studies demonstrating the promotion of PDL-like and mineralized tissues[1,2]. Additionally, MSCs have been extensively utilized in regenerative medicine, particularly in bone regeneration, in a variety of animal species, including sheep, cattle, pigs, and horses[3]. pUC-MSCs rich in MSCs offer the opportunity to study the complex interaction between cell passage and the biological properties of these cells in a context very closely related to potential large animal model manipulation applications[4]. To explore these biological potentials, these cells must retain their initial properties, such as stemness ability, during manipulation and *in vitro* culture.

Employing MSCs in regenerative medicine requires retaining their stemness properties after *in vitro* manipulation[5]. Maintenance of stemness in MSCs is crucial and is influenced by various factors, including culture conditions and cell passage[6]. Careful manipulation of culture conditions, including media composition, growth factors, and passage frequency influences the phenotype and behavior of MSCs[3]. The *in vitro* culture of these cells is not just a technical consideration but a fundamental aspect that determines their usefulness for therapeutic applications and the controlled environment is crucial for maintaining the effectiveness and functionality of MSCs[7]. Further studies suggest that improper culture or frequent passages may result in loss of stemness and adversely alter MSC properties[8,9]. In general, the maintenance of stemness in MSCs can be greatly impacted by the interaction of transcription factors, culture environment, and epigenetic modifications[10]. Therefore, the particular culture conditions needed to keep pluripotent stem cells (SCs) undifferentiated must also be considered.

Pigs are increasingly recognized as valuable animal models for stem cell research due to their anatomical and physiological similarities to humans[11]. Porcine tissues, such as the umbilical cord, are a readily available and ethically acceptable source of MSCs, which is essential for the development of cellular therapies.

The study examines MSCs from large animals like pUC-MSCs, which are ideal models for translational research due to their physiological similarities to human MSCs[12]. These similarities include comparable organ size, cardiovascular and immune systems and

metabolic rates, making pigs particularly relevant for translational research in regenerative medicine and transplantation. In addition, pigs have a relatively short gestation period and produce large litters, facilitating in-depth experimental studies. The pig represents an extraordinary model for the in vitro or in vivo study of MSCs in tissue regeneration[13]. The choice of pigs in our study is based on their closer genetic and physiological resemblance to humans compared to other large animals, which could provide more applicable insights into MSCs behavior and therapy[14–16]. Taken together, these factors make the pig an ideal model for advancing stem cell research and its use as large animal model for research[17]. The study explores the influence of the number of cell passages on the stemness and differentiation properties of pUC-MSCs, to use the pig as a model for handling large animals and limiting the constraints on the use of the human model.

Materials and methods

All the chemicals used in this study were procured from Sigma-Aldrich Co., Inc. (St. Louis, MO, USA). The immunocytochemistry analysis markers were purchased from Molecular Probes, Life Technologies, Thermo Fisher Scientific (Waltham, MA, USA).

Preparation of pUC-MSCs

To obtain pUC-MSCs, the fetal umbilical cords from pregnant sows were collected when delivered (12 h) from the pig breeding base farm and transported to the research laboratory within 2 h, and then the cords were placed in sterile phosphate-buffered saline (PBS) containing the antibiotics amphotericin B, penicillin, and streptomycin. A 5 cm long section of the umbilical cord tissue (UTC) was cut longitudinally to remove the umbilical arteries and veins. Subsequently, the UCT were cut into 2 mm × 2 mm pieces and transferred to plates containing Dulbecco's modified Eagle's medium (DMEM) supplemented with 15% fetal bovine serum (FBS). The cells grew out of the pieces and into cell clusters after 3 d. The medium was replaced after 5 d to prevent mechanical stress and replenished every 3 d. The cells were collected using accutase® (MP Biomedicals, USA) after 7–10 d, reaching 80% confluence, and reseeded at a rate of 3×10^5 approximately in a flask with a growth area of 25 cm^2 (T25). The cell suspension was collected by pipetting and centrifuged at 1,000 rpm for 2–3 min. The supernatant containing cells was transferred to separate tubes and centrifuged at 1,000 rpm for 5–10 min. The cell pellet was then washed at least three times. Isolated cells were suspended in a medium of DMEM, 15% FBS, and antibiotics and grown in a T25 cell culture flask at 37 °C, 5% CO_2, and high humidity. The pUC-MSCs were passed up to 11 passages.

Growth status and morphology of pUC-MSCs

Cells from passages 4 to 11 were cultured *in vitro* to assess growth characteristics. After reaching 70%–80% confluence, they were propagated using trypsin in DMEM with 15% FBS without antibiotics. Then pUC-MSCs morphology was visualized under an Olympus IX71 microscope at passages 4, 6, 9, and 11 when confluence reached 70%–80%. Subsequently, 0.3×10^6 pUC-MSCs per well were seeded in 6-well plates in culture medium (37 °C, 5% CO_2). After 48 h, the growth medium was replaced with a working solution consisting of DMEM and Cell Counting Kit-8 CCK-8 (Biosharp Life Science, BS350B, Heifei, Anhui, China) with a volume ratio 100:10. The plates were incubated for 4 h at 37 °C and 5% CO_2. A microplate reader (Biosharp Life Science) was used to measure the optical density of pUC-MSCs to quantify cell viability. Microscopic evaluation of cell morphology enabled a qualitative assessment of physical changes over successive passages cells from day 1 to day 12, with at least three replicated in each group. The population doubling time (PDT) was computed using the logarithmic increase in cell concentration equation. PDT is calculated as tlog2/log(Nt/N0), where Nt represents the number of cells during the culture period and N0 represents the initial cell number. Quantifying growth rates and viability provided insight into proliferative capacity and survival, allowing for a better understanding of cell growth and viability.

Immunocytochemistry

Immunocytochemistry of pUC-MSCs was performed to detect the MSCs marker CD90 (ThermoFisher Scientific; MA1-84601). Cells grown on coverslips to 60%–70% confluence were fixed with 4% paraformaldehyde and permeabilized with 0.3% Triton X-100 for intracellular staining. Nonspecific binding was blocked with 10% FBS. Cells were labeled with a CD90 primary antibody (1:500 dilutions) and a FITC-conjugated secondary antibody overnight at 4 °C. Nuclei were counterstained with hoechst33343 with 1 μg/mL in PBS for 15–20 min. Slides were mounted with ProLong Gold anti-fade reagent and imaged under a ZEISS fluorescence microscope. Control cells were subjected to identical staining procedures except for the primary antibody. After resuspension, cells were grown to around 60% confluence. All pUC-MSCs were verified by positive expression of CD90, and overlaid histograms for each cell marker and corresponding antibody isotype control were generated using Flowing Software (version 2.5.1). The population of pUC-MSCs positive was determined using a bivariate dot-plot with FLOWJOY software (Three Star, Ashland, OR, USA)

RNA sequencing

Total RNA was extracted from cells using TRIzol reagent (Invitrogen, Carlsbad, CA, USA) according to standard protocol. RNA quantity and integrity were verified using the Agilent 2100 Bio-analyzer. The sequencing library for each RNA sample was prepared using the Ion Total RNA-Seq v2 kit (Life Technologies, USA) according to the protocol provided by the manufacturer. Oligo (dT) beads were used to extract and enrich total mRNA. The enriched mRNA was reverse-transcribed and fragmented with random primers to produce cDNA. The cDNA fragments were purified using a QiaQuick PCR extraction kit (Qiagen, Venlo, The Netherlands). Following PCR amplification, TIANKE Biotechnology Co. Ltd's Illumina HiSeq TM 2500 (Hangzhou, China) was used for sequencing. Raw data (raw reads) in fastq format from the input RNA-seq data analysis libraries were first processed using in-house Perl scripts and clean data (clean reads) were obtained by removing reads of poor quality but including adapters and poly (N) from raw data. Meanwhile, the clean data's Q20, Q30, and GC contents were determined.

Bioinformatic analysis

The initial step in analyzing input RNA-seq data libraries involved processing raw data using internal Perl scripts. Low-quality reads with adapters were removed to retain high-quality reads. The GC content and Q20 and Q30 proportions were calculated for these filtered measurements. The cleaned measurements were aligned with the pig reference genome using the Bowtie2 algorithm (https://asia.ensembl.org/Sus_scrofa/Info/Index) using the Bowtie2 algorithm[18]. Gene expression was quantified using HTSeq-count (v0.6.1), which determined the number of reads aligned to each gene[19]. FPKM was calculated for each gene by considering the gene length and read counts mapped to that gene in HTSeqcount. P-values were adjusted using the Benjamini and Hochberg method to account for possible false discoveries[20,21]. Subsequently, genes with an FDR below 0.05 and a 2-fold difference between the two groups, as determined by DESeq2, were designated DEGs.

Furthermore, the R package vegan performed PCA on two sets of samples[22]. The R package statistics generated each gene's boxplots and correlation cluster heat maps. The DEG enrichment studies were conducted using the Top GO technique, focusing on GO and KEGG. Only results with a Q value less than 0.05 were considered significant. TIANKE Biotechnology Co., located in Hangzhou, China, conducted the sequencing and transcriptome analysis. Then, the interpretation of the results and the realization of heat map graphs and enrichment

analysis were generated by the bioinformatics tool SRPLOT, developed by bioinformatics.org.cn[23,24].

Quantity real-time PCR (qRT-PCR)

To prepare cell samples for RNA extraction, adherent cells were removed from the incubator and observed under the microscope to ensure good growth, then washed three times with PBS (preparation 0.1% Diethylpyrocarbonate-H20) at room temperature. The PBS was removed, and an appropriate amount of TRIzol was added (1 ml TRIzol for 1×10^7 cells) and then pipetted several times. Then, 3 ml of PBS (DEPC-H20 preparation) was added at room temperature and washed once. After pipetting several times, the cell layer should be wholly lysed by visual inspection. According to the manufacturer's instructions, total RNA was extracted from pUC-MSCs at 80%–90% confluence using TRIzol (Invitrogen, Carlsbad, CA). Then, HiScript® RT SuperMix for RT-PCR kit (Vazyme Biotech Co., Nanjing, China) was used to transcribe total RNA according to the manufacturer's instructions. qRT-PCR using AceQ® RT-PCR and SYBR® Green Master Mix (Vazyme Biotech Co., China) in a 20 µL reaction volume was used to quantify each mRNA level. The primers used for qRT-PCR are listed in Table 1. The $2^{-\Delta\Delta Cт}$ method was used to analyze the data after normalizing the relative gene expression to the reference genes[25].

Data analysis

All measurements were carried out with at least three replicates. Data were expressed as Mean with SDs. The Shapiro-Wilk test was used to assess the normality distribution. Statistical significance was determined using one-way ANOVA, followed by Tukey's post hoc test for multiple comparisons. Graph Prism version 8.0 (IBM, New York, USA) for Windows 13.0, and the graphs were drawn with this software. A $p < 0.05$ was considered to be significantly different.

Results

Morphological observation and growth curve analysis

The morphology of the cells shown in Fig. 1a is that cells formed a rhomboid shape after 4–5 d of culture, then a spindle-shaped monolayer with central oval nuclei after 10 d. The appropriate number of cells to analyze the growth curve was 3×10^4 in 2 mL of medium per well (Fig. 1b, c). The cells of P4, P6, P9, and P11 were cultured for 12 d until they reached confluence, and the cells' growth was recorded every 24 h. It can be seen from Fig. 1b that the growth curve of P4, P6, P9, and P11 cells is 'S'. On the 1st–3rd day, the cells belong to the latent period and grow slowly. The cells from the 3rd to the 6th day belong to the logarithmic growth stage; the growth rate is faster, and the convergence degree of the cells increases. The proliferation rate belongs to the 7–9-day stage platform. Culture viability was 95% for cell growth during P4 and P6 and significantly lower for P9 and P11.

Table 1. Primer sequences of target genes in qRT-PCR.

Gene name	Gene ID	Primer sequence	Product length (bp)
MYC	NM_001005154.1	F: AGCACAATTATGCAGCGCCC R: GACCCTGCCACTGTCCAACT	80
KRAS	XM_013993793.2	F: GGGAGAGAGGCCTGCTGAAA R: ACTCTTGCCTACGCCACCAG	71
APC	NM_001206430.1	F: TGGCAACTTCGGGTAACGGT R: GCCTTCGAGGAGCAGAGTGT	99
DPPA4	XM_005654065.3	F: ACCGGCCAACCTGATTCACA R: TCCAGTTTCCGGCCTTTGGT	81
GAPDH	XM043245356.3	F: TCGGAGTGAACGGATTTGGC R: TGCCGTGGGTGGAATCATAC	
NOTCH3	XM_021083631.1	F: ATGGTCTTCCCTTACCACCG R: ACGGTTGTCAATCTCCAGCA	108
MAPK8	XM_021073087.1	F: CAGTCTCCACCGCCTAGGTT R: GATCCCTCGCTGCTACCTGG	75
OCT4	MF955857.1	F: GGCTCCCCCATGCATTCAAA R: TCTCTCCCTAGCTCACCCCTT	80
SOX2	NM_001123197.1	F: GAGCGCCCTGCAGTACAACT R: CCCTGCTGCGAGTAGGACAT	87
NANOG	EF522119.1	F: ACGGTGGACCTGCAAGTAGT R: GCTGCTGAGTAACCCAGACT	92

Evaluation of pUC-MSCs by flow cytometric analysis

As shown in Fig. 2a–d, CD90-positive cell proliferation varied significantly between passages. The percentage of positive cells in passages P4 and P6 was significantly higher ($p < 0.05$) compared to passages P9 and P11. The four independent cultures of pUC-MSCs were tested by FACS analysis at passages 4, 6, 9, and 11 and the results were comparable. Uniformly high levels of CD90-positive markers were detected, with only 66% to 95.9% of cells alive in P4 and P6; and relatively low levels of CD90-positive markers detected with only 24.4% to 30.6% of cells alive. In P9 and P11. Moreover, the majority of cells also expressed CD90 (24.4%–95.9%) (Fig. 2b). It shows that almost all living single cells co-express the CD90 cell surface antigen. Subsequently, pUC-MSCs were verified by positive expression of the CD90 surface antigen marker, and the overlaid histograms for each cell marker and corresponding antibody isotype control were generated using Flowing Software (version 2.5.1). The CD90 histogram has two overlapping peaks, in contrast to the IgG1 histogram. Positive cells appear as a distinct population on a light scatter plot or fluorescence histogram. Negative cells have minimal fluorescence, while positive cells have higher fluorescence, forming a distinct peak (Fig. 2b). A positive population of cells expressing CD90 is indicated by both peaks. Furthermore, this positive population is highlighted by the blue rectangle.

Transcriptomic analysis of pUC-MSCs

Subsequently, 12 libraries (MPS-P4-1, MPS-P4-2, MPS-P4-3, MPS-P6-1, MPS-P6-2, MPS-P6-3, MPS-P9-1, MPS-P9-2, MPS-P9-3, MPS-P11-1, MPS-P11-2, and MPS-P11-3) from cells were constructed for RNA-sequencing. The porcine reference genome maps approximately 98% matched the clean reads (version, Sus scrofa 11.1). The total rate of mapped reads was 94.32 to 98.41%, with a read rate of 38,952,882 to 39,323,628, and the proportion of mapped paired-end reads was. 83.7 to 86.9% (Table 2).

Identification of DEGs in all data sets

The coefficients of the multiple samples had significantly greater values within the same group than the other two groups. Three groups were identified for the principal component analysis (PCA) genes. Consequently, the reliability and repeatability of the sequencing data were high. With the volcano plot, 1,700 DEGs, including 1,073 up-regulated and 627 down-regulated DEGs, were identified in P6 vs P4. For P9 vs P4, a total of 923 DEGs, including 326 up-regulated and 597 down-regulated, were reported. For P11 vs P4, 175 significant DEGs were detected, including 59 up-regulated and 116 down-regulated genes (Fig. 3a, b). As shown in Fig. 3c, DEGs in the pUC-MSCs (P4, P6, P9, and P11) were hierarchically grouped into four distinct clusters, demonstrating a considerable difference in the pUC-MSCs expression profile as the passages progress P4, P6, P9, and P11 respectively.

GO and KEGG enrichment analysis of DEGs between groups of pUC-MSCs

KEGG and GO analysis of differentially expressed genes was conducted to understand better the differences in P4, P6, P9, and P11 of pUC-MSCs. The top 20 KEGG pathways in pairwise comparison are displayed in Fig. 4a–c respectively. The study analyzed various cell generation pathways, including stem cell stemness, differentiation, MAPK signaling, hepatitis C pathways, cell senescence, complement and coagulation

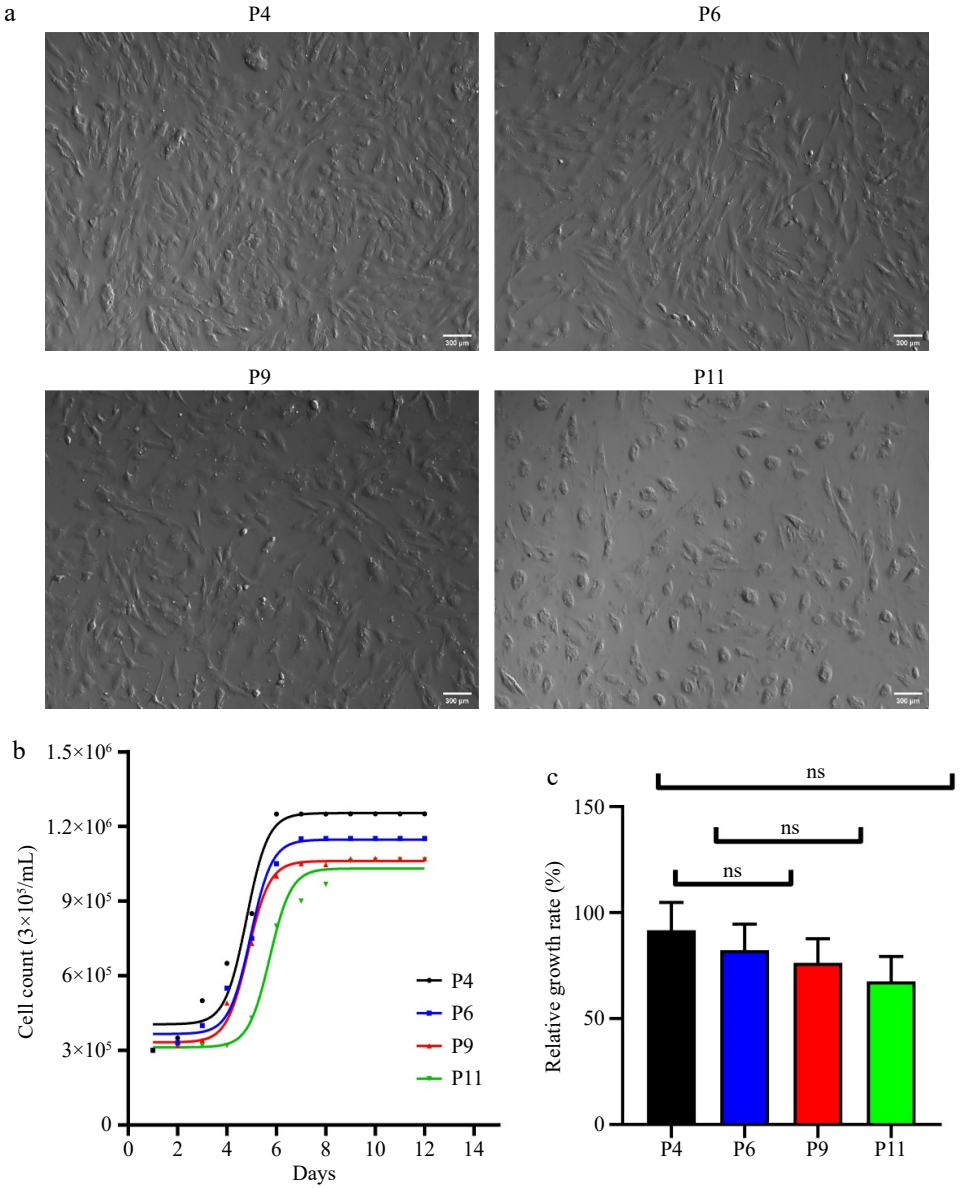

Fig. 1 Developmental status of pUC-MSC. (a) Cell morphology of pUC-MSC cultured at different passages (× 100) (bar = 300 μm); (b) Growth curve of pUC-MSC at passages 3, 6, and 9; (c) Relative growth rate. Different symbols (*, **, ***, ns) indicate significant differences among groups ($p < 0.05$).

Table 2. Mapping results with pig genome.

Sample	Reads number	Base number (bp)	Q20 (%)	Q30 (%)
MPS-P4-1	39,132,268	5,830,212,150	98.22	94.95
MPS-P4-2	39,384,712	5,894,408,375	98.41	95.34
MPS-P4-3	39,323,628	5,887,845,684	98.31	95.17
MPS-P6-1	39,279,880	5,877,249,370	98.17	94.75
MPS-P6-2	39,267,936	5,879,963,739	98.17	94.79
MPS-P6-3	39,248,876	5,872,768,921	98.12	94.67
MPS-P9-1	39,230,388	5,870,955,649	98.06	94.53
MPS-P9-2	39,317,102	5,885,981,291	98.3	95.12
MPS-P9-3	39,102,492	5,853,218,947	98.18	94.91
MPS-P11-1	39,078,322	5,849,103,924	98.25	94.97
MPS-P11-2	39,196,888	5,868,142,702	98.02	94.32
MPS-P11-3	38,951,882	5,831,153,453	98.32	95.18

cascades, transcriptional misregulation in cancer, and steroid biosynthesis. The most significant pathways were stem cell stemness, differentiation pathways, MAPK signaling pathways, metabolic pathways, PI3K-AKT signaling pathway, Hepatitis C, and terpenoid backbone biosynthesis, with genes up-regulated. The least significant pathways were the P53 Signaling pathway, autophagy, BMP signaling pathway, and Wnt signaling pathway. The most significant genes were filtered using *p*-value ($p < 0.05$).

KEGG and Go pathway enrichment analysis of DEGs for stemness, cell differentiation, and metabolic pathways

Five significant genes were selected for pathway discussion, with their genetic distribution described through KEGG enrichment analysis. Additionally, the roles of both positively and negatively regulated DEGs were investigated using GO enrichment analysis. The study highlighted several critical genes associated with stem cell stemness, including *DPPA4, SMAD5, MYC, APC,* and *KRAS*. DEGs for P6 compared to P4 revealed significant enrichment for 46 GO items (Fig. 5a). And 46 GO entries had significantly enriched DEGs for P9 and P4 (Fig. 5b). DEGs for P11 compared to P4 revealed a considerable enrichment for 45 GO items (Fig. 5c). The Expression Patterns reveal that P4 and P6 exhibited significantly higher expression levels of the aforementioned genes, indicating a robust stemness state. In contrast to groups of P4 and P9,

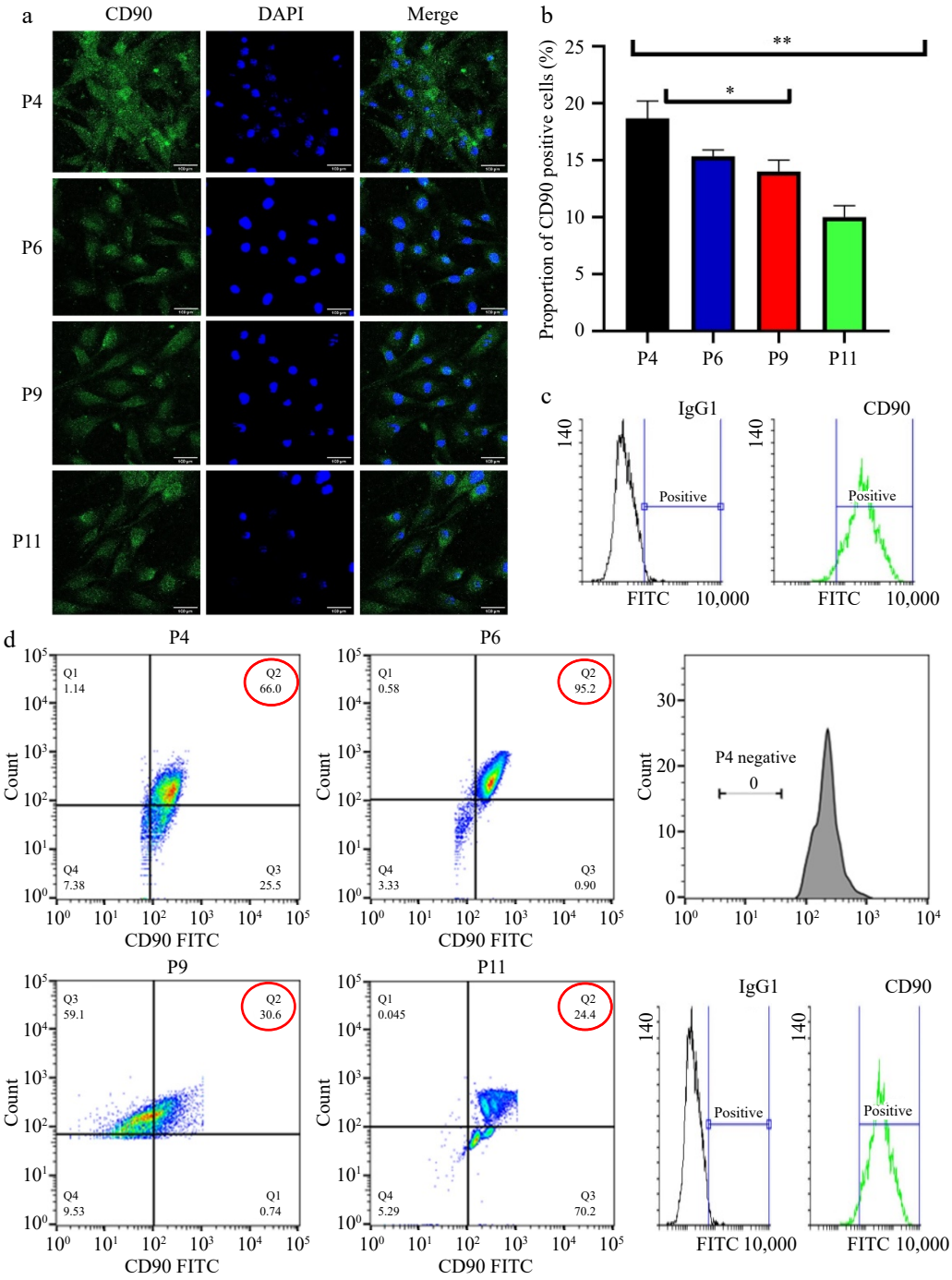

Fig. 2 Characterization pUC-MSC (a) Immunofluorescence and observation of cells incubated with CD90; DAPI is used for nuclear staining (b) Proportion of CD90 positive cells; (c) Flow cytometry for surface antigen marker (bar = 100 μm). Different symbols (*, **, ***, ns) indicate significant differences among groups ($p < 0.05$). (d) Flow cytometry analysis of pUC-MSCs; Dot-plot analysis expressing positive MSC-specific antigens CD90.

groups of P6 and P11 showed higher expression of genes related to stemness of stem cells (SCs), including *FZD6, BMPRIA, APC, ZNF518A, RIFI, PCGF5, SMARCADI, KRAS, G2E3, SMAD3, STAC2, ACVR2B, WNT6, FGRLI, FZD9,* and *CRLFI*) (Fig. 5a). For instance, the *APC* gene showed a twofold increase in expression in P6 compared to P4, P9, and P11, making P6 an optimal stage for maintaining stemness. In contrast, the expression of P9 and P11 stemness markers was notably lower in later passages, indicating a decline in stemness characteristics as the cells age. This suggests that the regulatory mechanisms governing stemness are more active in earlier passages.

In cell differentiation pathway genes such as *NOTCH3, JAK3*, and *MAPK8* were analyzed for their roles in differentiation. The expression of differentiation-related genes varied significantly across passages. For example, genes associated with the *NOTCH* signaling pathway, which is vital for cell fate determination, showed increased expression in later passages, indicating a potential shift towards differentiation as the cells progress from P4 to P11. The expression of genes related to cell differentiation, such as *NOTCH3, CRLFI, JAK3, MAPK8*, and *NFKTC4*, was upregulated at passages P4 and P11 (Fig. 6a). Conversely, *PPP3CA, SMAD3*, and *NFAT5* were down-regulated. *NFKBIA* and *SLA-DQAI* showed upregulation at P9 (Fig. 6b). Genes like *FASN, LSS, MVD, EBP, PGP, TKI, PIK3C3, AGPS, PIK3CA, ATP8, COX3*, and *ATP6* were upregulated at passages P4 and P6, while *DEGS2* and *PAPSSI* exhibited downregulation. *FAH, HSD17B8,*

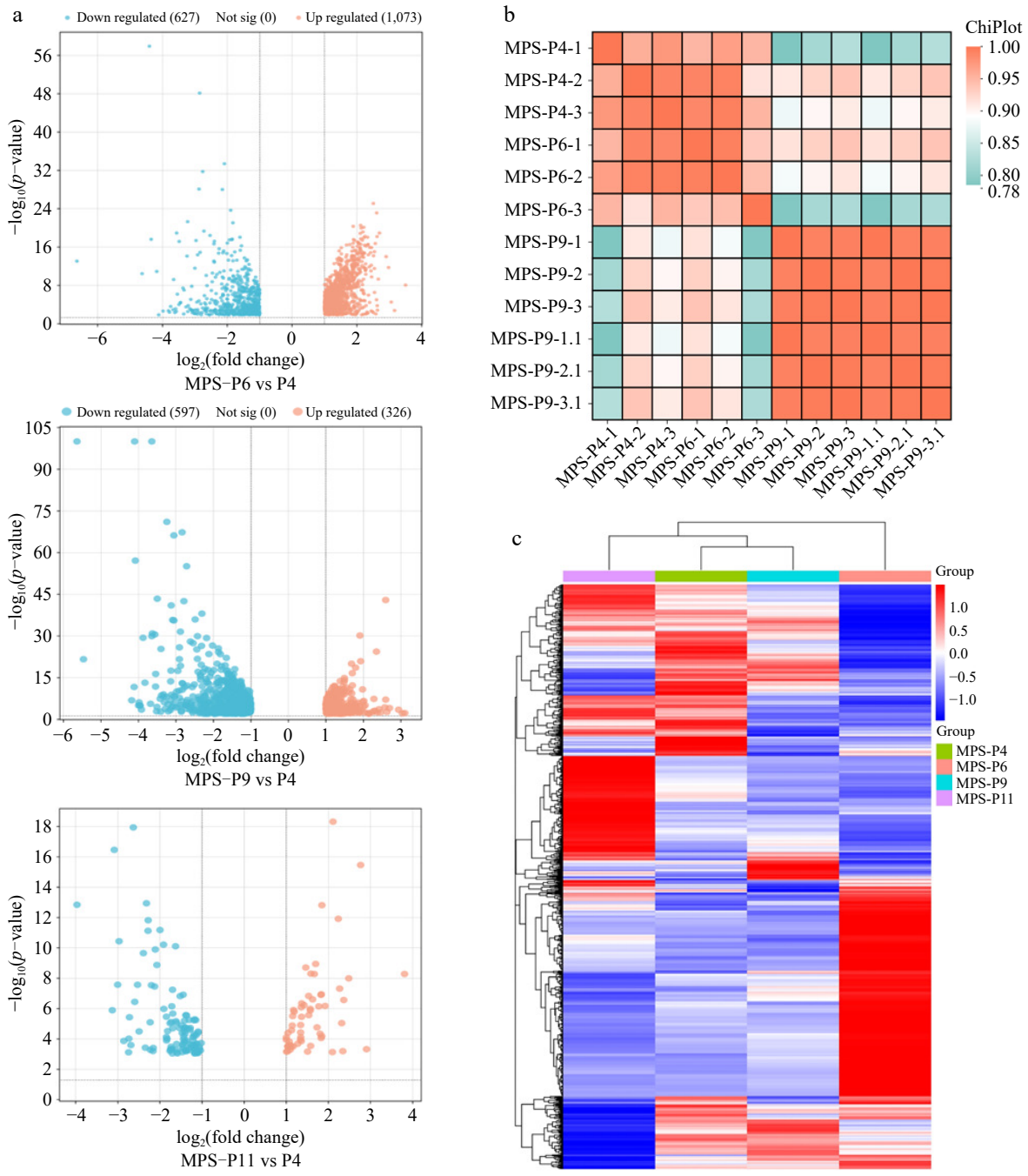

Fig. 3 The overall distribution of transcripts in three data sets. (a) Pearson correlation heatmap showing the correlation between all sample data sets. (b) Volcano plot of significant DEGs detected from three data sets. (c) Heatmaps show the overall distribution of DEGs in respective data sets.

B4GALNT4, and *ENOI* were upregulated at P4 and P11 but downregulated at P6 (Fig. 6c). At the cellular senescence level, genes *SMAD3, IGFBP2, SERPINE1, IGFBP6, FOXO1*, and *ETS2* were upregulated at P11 and downregulated at P4, P6, and P9. On the other hand, genes *CHEK1, CCNE2, RBL1, CCNJ, PTEN, TRPM7, SIRT1, ATR, NFAT5, ATM, KRAS*, and *NBN* were upregulated at passage P6 and downregulated at P4, P9, and P11 (Fig. 6d). This shift suggests that while early passages are more conducive to maintaining stemness, later passages may be more geared towards differentiation, which is essential for tissue engineering applications.

Thus, most of the significantly down-regulated DEGs in P11 compared to P6 examined using GO enrichment were related to metabolic, developmental, and single-organism processes. In metabolic pathways, which are essential for providing the energy and building blocks necessary for cell growth and function the expression patterns show that many DEGs related to metabolic processes were found to be down-regulated in later passages (P9 and P11) compared to earlier passages (P4 and P6). This down-regulation may indicate a shift in cellular metabolism as the cells age, potentially affecting their viability and functionality. The study suggests that maintaining a high metabolic rate in early passages is crucial for supporting the high proliferation rates and stemness characteristics of pUC-MSCs.

Detection of DEGs by qRT-PCR

Firstly, the study validated the expression of several genes (*APC, MYC, KRAS, SMAD5*, and *DPPA4)* crucial in regulating stemness of stem cells. This confirms the importance of these genes in the context of

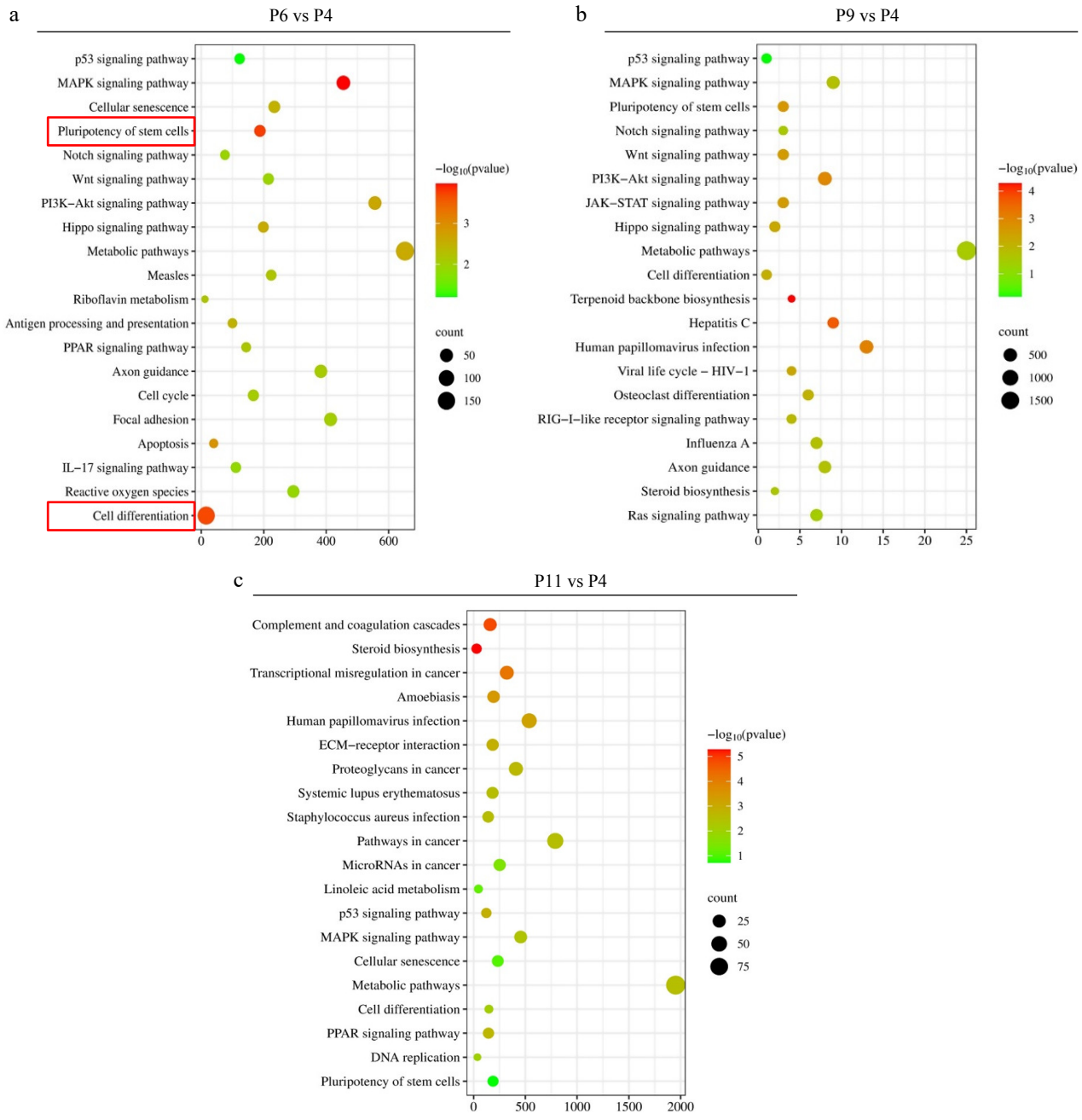

Fig. 4 KEGG enrichment analysis of DEGs in the different comparison groups, where the X-axis represents DEG's numbers and the Y-axis represents the pathway. (a) P6 vs P4, (b) P9 vs P4, and (v) P11 vs P4.

pUC-MSCs. The *APC* gene exhibits significantly higher expression levels in P6 than in P4, P9, and P11, with a twofold increase in P6. However, the expression of the *APC* gene in P9 and P11 did not show statistically significant differences (Fig. 7a). On the other hand, the *MYC* and *DPP4* genes are highly expressed in P11, with no significant differences observed in their expression levels between P6 and P9 (Fig. 7b–d). Additionally, the *KRAS* and *SMAD5* genes are highly expressed in P6, with *KRAS* showing non-significant results in P6 (Fig. 7c, d).

Finally, statistically significant differences were observed between the groups for *NOTCH3, MAPK8, OCT4, SOX2*, and *NANOG* expression ($p < 0.05$) for most comparisons (Fig. 8). Tukey's post hoc test further indicated that the significant differences predominantly occurred between P4 and P9 and P11, consistent with the hypothesis that these cells were losing stemness and initiating differentiation. These results highlight the regulatory shifts in gene expression that accompany the transition from stemness to differentiation, with decreased expression of key stemness markers (*OCT4, SOX2, NANOG*) and increased differentiation markers (*MAPK8*) in higher passage cells (P9, P11). Additionally, the decline in *NOTCH3* expression points to a loss of signaling that supports stem cell maintenance in these later stages.

These PCR results complement the transcriptomic analysis and contribute to an improved understanding of gene expression changes associated with stemness in pUC-MSCs. This deeper understanding enhances the potential applications of these cells in regenerative medicine and tissue engineering.

Discussion

MSCs can be derived from various tissues, but MSCs isolated from umbilical cords offer significant advantages over those obtained from

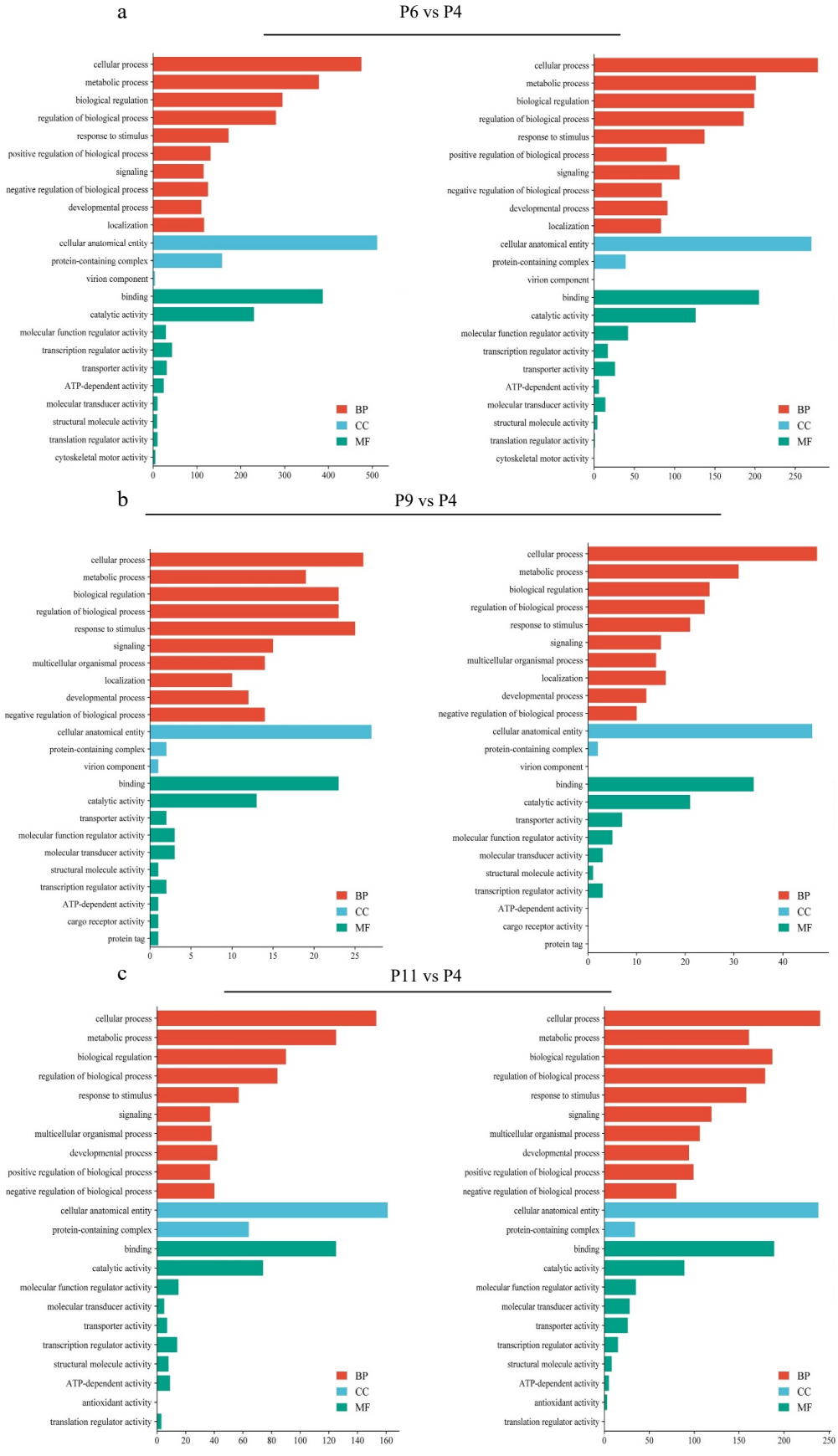

Fig. 5 GO enrichment analysis of DEGs in different comparison group, where the X-axis represents the number of DEGs and the Y-axis represents different GO terms. (a) P6 vs P4, (b) P9 vs P4, and (c) P11 vs P4.

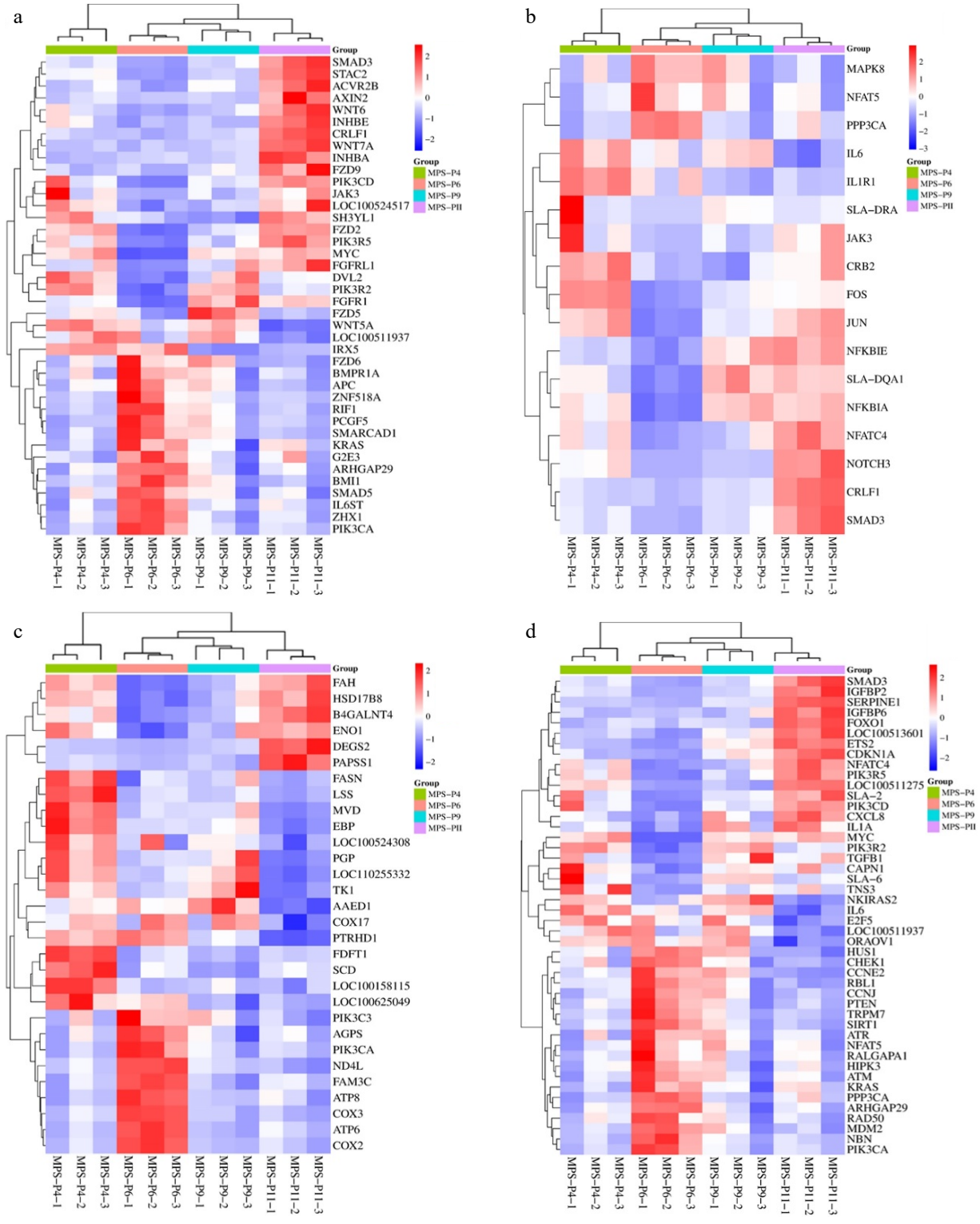

Fig. 6 Comparison of P4, P6, P9, and P11 transcriptome profiles. The cluster heatmap analysis of differentially expressed related to (a) stemness, (b) cell differentiation, (c) metabolic pathways, and (d) cells cellular senescence.

other sources. These advantages include non-invasive collection (since the umbilical cord is typically discarded after birth), reduced risk of contamination, and a higher initial cell yield, particularly from the cord lining, compared to other cord tissues[26]. In this study, it was observed that MSCs at passages P4 and P6 exhibited greater viability and stemness than those at P9 and P11. Similar trends have been reported in mouse studies, where MSCs derived from the umbilical vein showed typical fibroblastic morphology when observed under phase-contrast microscopy[27,28]. Proliferation capacity was measured as the time required for pUC-MSCs to complete one division cycle. Cells typically entered a lag phase during the first 1–3 d, where they adhered to the plate surface before beginning exponential division. The logarithmic growth phase occurred over the next 3–6 d, characterized by rapid cell proliferation in a stable environment with sufficient space. Growth plateaued between days 6–9 as space became limited, slowing cell division due to contact inhibition, a feature consistent with previous findings[29].

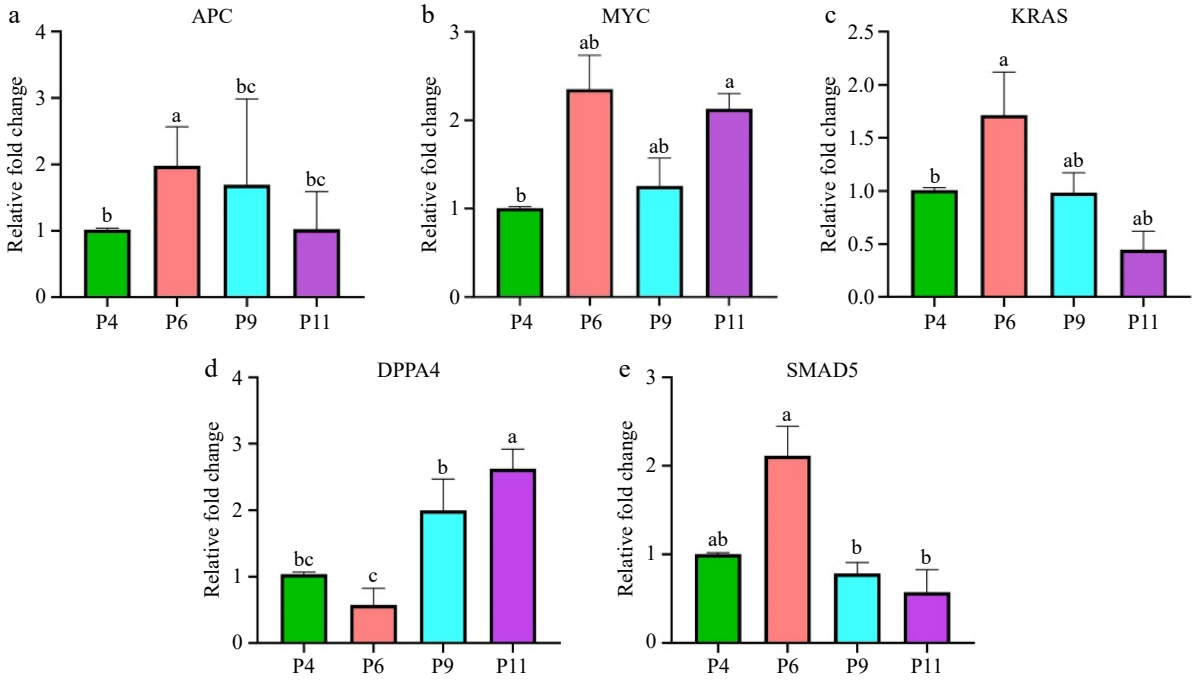

Fig. 7 Expression levels of pluripotency-related genes in pUC-MSC at P4, P6, P9, and P11. (a) *APC*, (b) *MYC*, (c) *KRAS*, (d) *DPPA4*, (e) *SMAD5*. Different symbols (a, b, c, d) which are on the top of each column indicate significant differences among groups ($p < 0.05$).

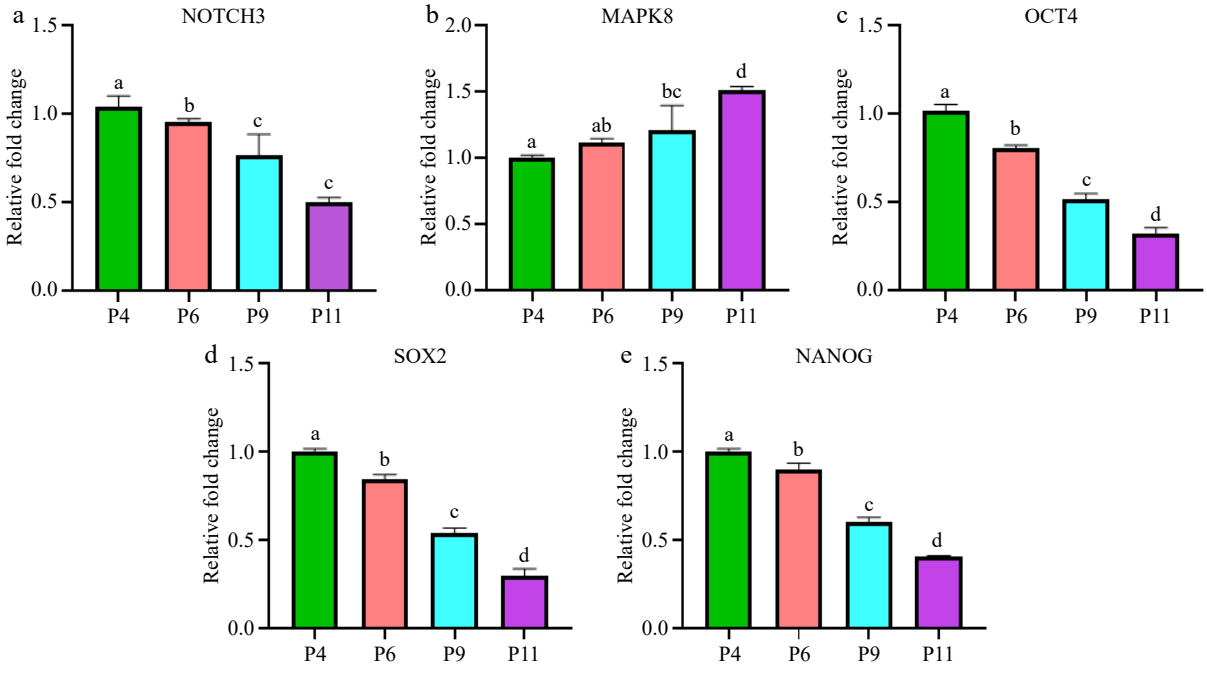

Fig. 8 Expression levels of differentiation related genes in pUC-MSC at P4, P6, P9, and P11. (a) *NOTCH3*, (b) *MAPK8*, (c) *OCT4*, (d) *SOX2*, (e) *NANOG*. Different symbols (a, b, c, d) which are on the top of each column indicate significant differences among groups ($p < 0.05$).

MSC proliferation capacity diminishes over successive passages, and our results demonstrated a significant difference in cell proliferation rates between passages P4, P6, P9, and P11. All passages exhibited an S-shaped growth curve, with P4 and P6 having shorter doubling times compared to P9 and P11 (averaging 33.87 h). These findings align with previous research on bone marrow and adipose-derived MSCs from Mongolian sheep, where doubling times were approximately 31 and 30 h, respectively[30–32]. MSCs from fetal sources, such as umbilical cord blood or Wharton's jelly, tend to have even shorter doubling times compared to adult-derived MSCs, reflecting their more primitive nature[33]. This typical feature of MSCs was thought to signify their more primitive character than adult stromal cells. The ability to form clones and cell colonies from a single cell is an important selection criterion and evidence of the ability to replenish its population, a crucial feature of SCs[33]. While UC-MSCs from humans and other animals have been extensively studied, pUC-MSCs represent a valuable model for large animal manipulation to mimic human cures so as to reduce the required number of non-human primate research due to the physiological similarities between pigs and humans. Our data further emphasize the importance of considering species-specific characteristics. The shorter doubling times

observed in early passage pUC-MSCs are similar to human UC-MSCs[34].

The ability of MSCs to form colonies from single cells is a critical feature of SC populations, indicating their capacity for self-renewal. This feature is particularly pronounced in early-passage cells, as demonstrated by our findings that early passage MSCs maintained high CD90 expression, a surface marker for MSCs[35,36]. Further evaluation of stemness was conducted through immunofluorescence staining, which revealed the persistence of stemness-associated markers such as CD90 across passages. This consistency suggests that early-passage MSCs retain their stem-like characteristics[37]. For example, a study on human Wharton's jelly-derived MSCs found that early passages (P1–P5) exhibited superior proliferation and maintained their stem-like properties, while later passages showed diminished proliferative capacity and increased senescence markers[38]. It is noted that pUC-MSCs are characterized by the presence of cell-surface markers specific to the CD90 marker.

On a molecular level, various signaling pathways play crucial roles in maintaining stemness and controlling differentiation. Leukemia Inhibitory Factor (LIF) promotes stem cell maintenance in mice through the induction of *SOCS3*, which modulates the JAK-STAT pathway[39,40]. Key transcription factors such as *Oct4, Sox2*, and *Nanog* are indispensable for preserving MSC stemness, and their expression declines with increasing passage numbers[41]. Our data confirm that genes involved in maintaining stemness, including *DPPA4, SMAD5, MYC, APC*, and *KRAS* were highly expressed in early passages (P4 and P6), reinforcing the idea that these early-stage cells are more stemness[42,43]. Stemness features persist across numerous generations[44].

Research on human bone marrow-derived MSCs shows that early passages (up to P6–P8) maintain a stable phenotype, characterized by consistent morphology, surface marker expression, and stemness marker levels[45]. In the present study, early passage, the pUC-MSCs showed strong expression of stemness markers like *Oct4, Sox2*, and *Nanog*, further validating their stemness. As passage numbers increased, however, these markers diminished, signaling a decline in the cells' stem-like properties[45,46]. These findings align with prior studies on MSCs from other species, which indicate that increased passages result in diminished stemness and heightened differentiation markers[47]. Their reduced activity in later passages suggests a down-regulation of stemness and an increase in genes associated with cellular aging and differentiation.

The preservation of stemness is closely linked to complex interactions between multiple genes and the modulation of key signaling pathways. In particular, the *NOTCH3*, *JAK3*, and *MAPK8* pathways play pivotal roles in regulating stem cell fate, stress responses, and apoptosis, which ultimately influence stemness[48]. *NOTCH3* activation has been shown to promote self-renewal and stemness in various stem cell systems[49]. Similarly, the inhibition of *JAK3* has been shown to prevent differentiation by blocking the activation of pro-differentiation signals[50]. Additionally, *MAPK8* is a key regulator of apoptosis; inhibiting this pathway prolongs stemness by reducing stress-induced cell[51,52]. Moreover, metabolic rewiring, particularly the shift between glycolysis and oxidative phosphorylation (OXPHOS), plays a crucial role in stem cell maintenance. Stemness primarily relies on glycolysis even under oxygen-rich conditions, a phenomenon known as the Warburg effect. A switch to OXPHOS is typically associated with differentiation. By promoting glycolysis and suppressing OXPHOS, it is possible to prolong the stemness of MSCs[53–55]. Key enzymes such as hexokinase 2 (HK2), regulated by c-Myc, are critical for sustaining this metabolic profile[55].

This study highlights the complex interplay between gene expression, metabolic regulation, and signaling pathways in maintaining MSC stemness across different passages. Early-passage (P4 and P6) of pUC-MSCs showed higher expression of stemness-related genes such as *DPPA4, SMAD5, MYC, APC*, and *KRAS*, suggesting that these genes play a critical role in maintaining stemness. As pUC-MSCs undergo further passages, alterations in metabolic and signaling pathways lead to a gradual decline in stemness and the initiation of differentiation processes.

Conclusions

The pUC-MSCs were isolated and cultured with fibroblast-like morphology and high proliferative capacity. Preliminary analyses revealed a higher level of expression of the stemness marker CD90 in pUC-MSCs at P4 and P6. By analyzing the transcriptome, the study concludes that P4 and P6 generations are the optimal stages to use for stemness cell therapy in pUC-MSCs, as the key genes associated with stem cell stemness are more likely to be up-regulated in early stages (P4 and P6) than in late stages (P9 and P11). Furthermore, the expression of *SOX2*, a key gene known to regulate stem cell stemness, is significantly up-regulated in the P4 and P6 generations. The modulation of metabolic pathways, coupled with the introduction of inhibitors or agonists targeting key signaling pathways such as *NOTCH3, JAK3*, and *MAPK8*, represents a promising approach to prolonging stemness in SCs. By maintaining glycolytic flux, preventing external differentiation signals, and reducing stress-induced apoptosis, these strategies could significantly extend the use of stemness in regenerative medicine. Future studies should focus on optimizing these interventions to ensure the efficient and long-term maintenance of stemness in diverse stem cell systems. The findings of this study may facilitate the discovery of new genes involved in biological processes. Hence, this information could be valuable for improving and controlling stemness properties and understanding the regulatory mechanisms in differentiating SCs into specialized cells.

Ethical statement

The data used in this study were provided by group research and collected from previously published sources. Therefore, no animal care or animal ethics committee approval was required for this study.

Author contributions

The authors confirm contribution to the paper as follows: conceptualization, methodology: Koutonin BOM, Li J; investigation, validation: Koutonin BOM, Jiang Y, Saeed HA, Zhang F; software, data collection, writing - draft manuscript preparation: Koutonin BOM; visualization, writing - manuscript revision: Jiang Y, Saeed HA, Zhang F; resources: Koutonin BOM, Li J; supervision, project administration, funding: Li J. All authors reviewed the results and approved the final version of the manuscript.

Data availability

The data used in this study were provided by group research and collected from previously published sources.

Acknowledgments

The present study was supported by Jiangsu Key R&D plan (Modern Agricultural) (Grant No. BE2021352) and Jiangsu Agriculture Science and Technology Innovation Fund (JASTIF) (Grant No. CX (21)3132) and JBGS project of Seed Industry Revitalization in Jiangsu Province (JBGS (2021)026).

Conflict of interest

The authors declare that there is no conflict of interest. Juan Li is the Editorial Board member of *Animal Advances* who was blinded from reviewing or making decisions on the manuscript. The article was subject to the journal's standard procedures, with peer-review handled independently of this Editorial Board member and the research groups.

References

1. Lotfy A, Salama M, Zahran F, Jones E, Badawy A, et al. 2014. Characterization of mesenchymal stem cells derived from rat bone marrow and adipose tissue: A comparative study. *International Journal of Stem Cells* 7:135–42
2. Kamiya D, Takenaka-Ninagawa N, Motoike S, Kajiya M, Akaboshi T, et al. 2022. Induction of functional xeno-free MSCs from human iPSCs via a neural crest cell lineage. *NPJ Regenerative Medicine* 7:47
3. Li M, Chen H, Zhu M. 2022. Mesenchymal stem cells for regenerative medicine in central nervous system. *Frontiers in Neuroscience* 16:1068114
4. Pan Q, Fouraschen SMG, de Ruiter PE, Dinjens WNM, Kwekkeboom J, et al. 2014. Detection of spontaneous tumorigenic transformation during culture expansion of human mesenchymal stromal cells. *Experimental Biology and Medicine* 239:105–15
5. Wang F. 2006. Culture of Animal Cells: A Manual of Basic Technique, Fifth Edition. *In Vitro Cellular & Developmental Biology - Animal* 42:169
6. Tsai CC, Chen YJ, Yew TL, Chen LL, Wang JY, et al. 2011. Hypoxia inhibits senescence and maintains mesenchymal stem cell properties through down-regulation of E2A-p21 by HIF-TWIST. *Blood* 117:459–69
7. Sensebé L, Bourin P. 2009. Mesenchymal stem cells for therapeutic purposes. *Transplantation* 87:S49–S53
8. Kamenaga T, Kuroda Y, Nagai K, et al. 2021. Cryopreserved human adipose-derived stromal vascular fraction maintains fracture healing potential via angiogenesis and osteogenesis in an immunodeficient rat model. *Stem Cell Research & Therapy* 12:110
9. Marquez-Curtis LA, Elliott JAW. 2024. Mesenchymal stromal cells derived from various tissues: biological, clinical and cryopreservation aspects: Update from 2015 review. *Cryobiology* 115:104856
10. Hu C, Li L. 2015. *In vitro* culture of isolated primary hepatocytes and stem cell-derived hepatocyte-like cells for liver regeneration. *Protein & Cell* 6:562–74
11. Kobayashi E, Hishikawa S, Teratani T, Lefor AT. 2012. The pig as a model for translational research: overview of porcine animal models at Jichi Medical University. *Transplantation Research* 1:8
12. Shih BB, Brown SM, Barrington J, Lefevre L, Mabbott NA, et al. 2023. Defining the pig microglial transcriptome reveals its core signature , regional heterogeneity , and similarity with human and rodent microglia. *Glia* 71:334–49
13. Feng Z, Yang Y, Liu Z, Zhao W, Huang L, et al. 2021. Integrated analysis of DNA methylome and transcriptome reveals the differences in biological characteristics of porcine mesenchymal stem cells. *BMC Genomic Data* 22:56
14. Boucard N, Viton C, Agay D, Mari E, Roger T, et al. 2007. The use of physical hydrogels of chitosan for skin regeneration following third-degree burns. *Biomaterials* 28:3478–88
15. Conrad JV, Meyer S, Ramesh PS, Neira JA, Rusteika M, et al. 2023. Efficient derivation of transgene-free porcine induced pluripotent stem cells enables *in vitro* modeling of species-specific developmental timing. *Stem Cell Reports* 18:2328–43
16. Kahveci R, Kahveci Z, Sirmali S, Özcan M. 1995. Urethral reconstruction with autologous vein graft: an experimental study. *British Journal of Plastic Surgery* 48:500–3
17. Vodička P, Smetana K Jr, Dvořánková B, Emerick T, Xu YZ, et al. 2005. The miniature pig as an animal model in biomedical research. *Annals of the New York Academy of Sciences* 1049:161–71
18. Langmead B, Salzberg SL. 2012. Fast gapped-read alignment with Bowtie 2. *Nature Methods* 9:357–59
19. Cao M, Wang X, Guo S, Kang Y, Pei J, et al. 2022. F1 male sterility in Cattle-Yak examined through changes in testis tissue and transcriptome profiles. *Animals* 12:2711
20. Jafari M, Ansari-Pour N. 2019. Why, when and how to adjust your P values? *Cell Journal* 20:604–607
21. Chen X, Sarkar SK. 2020. Benjamini – Hochberg procedure applied to mid p-values. *Journal of Statistical Planning and Inference* 205:34–45
22. Brownstein CA, Beggs AH, Homer N, Merriman B, Yu TW, et al. 2014. An international effort towards developing standards for best practices in analysis, interpretation and reporting of clinical genome sequencing results in the CLARITY Challenge. *Genome Biology* 15:R53
23. Guan D, Tian H. 2017. Integrated network analysis to explore the key genes regulated by parathyroid hormone receptor 1 in osteosarcoma. *World Journal of Surgical Oncology* 15:177
24. Fan M, Jin C, Li D, Deng Y, Yao L, et al. 2023. Multi-level advances in databases related to systems pharmacology in traditional Chinese medicine: a 60-year review. *Frontiers in Pharmacology* 14:1289901
25. Livak KJ, Schmittgen TD. 2001. Analysis of relative gene expression data using real-time quantitative PCR and the $2^{-\Delta\Delta CT}$ method. *Methods* 25:402–8
26. Hass R, Kasper C, Böhm S, Jacobs R. 2011. Different populations and sources of human mesenchymal stem cells (MSC): A comparison of adult and neonatal tissue-derived MSC. *Cell Communication and Signaling* 9:12
27. Yang Y, Zhang W, Wang X, Yang J, Cui Y, et al. 2023. A passage-dependent network for estimating the in vitro senescence of mesenchymal stromal/stem cells using microarray, bulk and single cell RNA sequencing. *Frontiers in Cell and Developmental Biology* 11:998666
28. Cárdenas AO, Zamora-Rodríguez BC, Batalla-García KA, Ávalos-Rodríguez A, Contreras-Ramos A, et al. 2023. Isolation and identification of mesenchymal stem cells derived from adipose tissue of sprague dawley rats. *Journal of Visualized Experiment* 194:e65172
29. Geraerts M, Verfaillie CM. 2009. Adult Stem and Progenitor Cells. In *Engineering of Stem Cells. Advances in Biochemical Engineering/Biotechnology*. vol. 114. Berlin, Heidelberg: Springer. pp. 1–21. doi: 10.1007/10_2008_21
30. Fu X, Xu B, Jiang J, Du X, Yu X, et al. 2020. Effects of cryopreservation and long-term culture on biological characteristics and proteomic profiles of human umbilical cord-derived mesenchymal stem cells. *Clinical Proteomics* 17:15
31. Su X, Ling Y, Liu C, Meng F, Cao J, et al. 2015. Isolation, culture, differentiation, and nuclear reprogramming of Mongolian sheep fetal bone marrow-derived mesenchymal stem cells. *Cellular Reprogramming* 17:288–96
32. Tian Y, Tao L, Zhao S, Tai D, Liu D, et al. 2016. Isolation and morphological characterization of ovine amniotic fluid mesenchymal stem cells. *Experimental Animals* 65:125–34
33. Kajiyama S, Nagashima Y, Funatsu T, Suzuki T, Fukaya M, et al. 2021. Effects of conditioned medium from bone marrow cells on human umbilical cord perivascular cells. *Tissue Engineering Part A* 27:382–89
34. Ding DC, Chang YH, Shyu WC, Lin SZ. 2015. Human umbilical cord mesenchymal stem cells: A new era for stem cell therapy. *Cell Transplantation* 24:339–47
35. Zimmerlin L, Donnenberg VS, Rubin JP, Donnenberg AD. 2013. Mesenchymal markers on human adipose stem/progenitor cells. *Cytometry Part A* 83A:134–40
36. Zhang Q, Yi DY, Xue BZ, Wen WW, Lu YP, et al. 2018. CD90 determined two subpopulations of glioma-associated mesenchymal stem cells with different roles in tumour progression. *Cell Death & Disease* 9:1101
37. Su HL. 2012. Neural differentiation of embryonic stem cells: Role of FGFs. In *Stem Cells Cancer Stem Cells*, ed. Hayat M. vol. 198. Dordrecht: Springer. pp. 249–56. doi: 10.1007/978-94-007-2900-1_24
38. Silvano M, Miele E, Valerio M, Casadei L, Begalli F, et al. 2015. Consequences of simulated microgravity in neural stem cells: biological effects and metabolic response. *Journal of Stem Cell Research & Therapy* 5:289
39. Loizou JI, Oser G, Shukla V, Sawan C, Murr R, et al. 2009. Histone acetyltransferase cofactor Trrap is essential for maintaining the hematopoietic stem/progenitor cell pool. *Journal of Immunology* 183:6422–31
40. Poole CJ, van Riggelen J. 2017. MYC—master regulator of the cancer epigenome and transcriptome. *Genes* 8:142
41. Khoo MLM, Shen B, Tao H, Ma DDF. 2008. Long-term serial passage and neuronal differentiation capability of human bone marrow mesenchymal stem cells. *Stem Cells and Development* 17:883–96

42. Myers NE, Stokes MG, Nobre AC. 2017. Prioritizing Information during Working Memory: Beyond Sustained Internal Attention. *Trends in Cognitive Science* 21:449–61
43. VanRullen R. 2018. Attention Cycles. *Neuron* 99:632–34
44. Shan ZY, Wu YS, Li X, Shen XH, Wang ZD, et al. 2014. Continuous passages accelerate the reprogramming of mouse induced pluripotent stem cells. *Cellular Reprogramming* 16:77–83
45. Baouche M, Krawczenko A, Paprocka M, Klimczak A, Mermillod P, et al. 2023. Feline umbilical cord mesenchymal stem cells: Isolation and in vitro characterization from distinct parts of the umbilical cord. *Theriogenology* 201:116–25
46. Shi G, Jin Y. 2010. Role of Oct4 in maintaining and regaining stem cell pluripotency. *Stem Cell Research & Therapy* 1:39
47. Zhou L, Wang J, Huang J, Song X, Wu Y, et al. 2022. The role of mesenchymal stem cell transplantation for ischemic stroke and recent research developments. *Frontiers in Neurology* 13:1000777
48. Kyttälä A, Moraghebi R, Valensisi C, Kettunen J, Andrus C, et al. 2016. Genetic variability overrides the impact of parental cell type and determines iPSC differentiation potential. *Stem Cell Reports* 6:200–12
49. Andersson ER, Sandberg R, Lendahl U. 2011. Notch signaling: Simplicity in design, versatility in function. *Development* 138:3593–612
50. Jin W. 2020. Role of JAK/STAT3 signaling in the regulation of metastasis, the transition of cancer stem cells, and chemoresistance of cancer by epithelial–mesenchymal transition. *Cells* 9(1):217
51. Kyriakis JM, Avruch J. 2012. Mammalian MAPK signal transduction pathways activated by stress and inflammation: A 10-year update. *Physiological Reviews* 92:689–737
52. Bennett BL, Sasaki DT, Murray BW, O'Leary EC, Sakata ST, et al. 2001. SP600125, an anthrapyrazolone inhibitor of Jun N-terminal kinase. *Proceedings of the National Academy of Sciences of the United States of America* 98:13681–86
53. Zhang J, Ratanasirintrawoot S, Chandrasekaran S, Wu Z, Ficarro SB, et al. 2016. LIN28 Regulates Stem Cell Metabolism and Conversion to Primed Pluripotency. *Cell Stem Cell* 19:66–80
54. Folmes CDL, Nelson TJ, Martinez-Fernandez A, Arrell DK, Lindor JZ, et al. 2011. Somatic oxidative bioenergetics transitions into pluripotency-dependent glycolysis to facilitate nuclear reprogramming. *Cell Metabolism* 14:264–71
55. Kondoh H, Lleonart ME, Gil J, Wang J, Degan P, et al. 2005. Glycolytic enzymes can modulate cellular life span. *Cancer Research* 65:177–85